Cluster variation approach to the Ising square lattice with two- and four-spin interactions

C. Buzano and M. Pretti
Dipartimento di Fisica del Politecnico di Torino and Istituto Nazionale di Fisica della Materia Corso Duca degli Abruzzi 24, 10129 Torino, Italy

(Received 22 October 1996)

The phase diagram of the Ising square ferromagnet with nearest-neighbor, next-nearest-neighbor, and four-spin (plaquette) interactions is investigated using the cluster variation method in the square approximation. A complete analysis in temperature is performed for the ferromagnetic, superantiferromagnetic, and frustrated region of the ground state. Particular attention is devoted to the role of the four-spin interaction. The most remarkable effect is the occurrence, in several regions of the interaction parameter space, of first-order transitions and sometimes reentrance phenomena. Critical and tricritical points are almost analytically determined. [S0163-1829(97)03722-3]

I. INTRODUCTION

The general properties of the Ising model on a square lattice with nearest-neighbor (J) and next-nearest-neighbor (K) interactions are relatively well known. Many authors have explored the possibility of a nonuniversal critical behavior, with a variety of techniques like finite-size scaling,[1] perturbation theory,[2] low-[3] and high-[4] temperature expansions, Monte Carlo simulations,[5–8] and coherent-anomaly method.[9] Recently, using the cluster variation method[12–14] (CVM), Moran-Lopez *et al.*[10,11] have obtained, for a range of values of $R \equiv K/J$, a first-order transition, while, for the same range, other authors had reported second order with critical exponents continuously varying with R. This interesting result has led us to consider a model with nearest-neighbor (J), next-nearest-neighbor (K), and four-spin (plaquette) (L) interactions, in order to carefully analyze the effect of the plaquette term on the occurrence of first-order transitions. The investigation has been carried out by means of the same method employed by Moran-Lopez *et al.* We have used the CVM in the square approximation. The same model had been previously studied with renormalization-group techniques[1,15–17] and by the coherent anomaly method,[18] never pointing out the presence of first-order transitions. For a vanishing nearest-neighbor (NN) interaction the model reduces to the exactly solved eight-vertex Baxter model,[19,20] allowing us to evaluate the errors introduced by the CVM square approximation. The paper is organized as follows. In Sec. II we introduce the model Hamiltonian and briefly recall the general steps of the CVM. The free energy in the square approximation and the stationarity conditions are also derived. In Sec. III we analyze the ground state and qualitatively describe the phase diagram. In Sec. IV we determine critical and tricritical points, making use of a Landau expansion. Section V is devoted to a detailed analysis of the temperature phase diagram, and to a series of comparisons with other results. Finally in Sec. VI some concluding remarks are presented.

II. THE MODEL AND THE CVM FREE ENERGY

We consider an Ising square lattice characterized by the Hamiltonian:

$$\mathcal{H} = -J \sum_{\langle i,j \rangle'} \sigma_i \sigma_j - K \sum_{\langle i,k \rangle''} \sigma_i \sigma_k - L \sum_{\langle i,j,k,l \rangle} \sigma_i \sigma_j \sigma_k \sigma_l , \tag{1}$$

where $\sigma_i = \pm 1$ is the spin variable at the ith lattice site. The symbol $\Sigma_{\langle i,j \rangle'}$ ($\Sigma_{\langle i,k \rangle''}$) indicates summation over all nearest- (next-nearest-) neighbors, while $\Sigma_{\langle i,j,k,l \rangle}$ indicates summation over four sites in every square (plaquette) of our lattice; J, K, L are interaction energies. The above model reduces to the Baxter model when $J=0$, and to the Ising model for $K=L=0$. We make the hypothesis $J>0$ (ferromagnetic nearest-neighbor interaction) but the sign of J is irrelevant towards the thermodynamic behavior. We shall analyze the phase transitions of this model in the square approximation of the cluster variation method (CVM).[12–14]

In the CVM the entropy of the system is approximated as a sum of suitably weighted cluster entropies relative to a set P' of maximal clusters and their subclusters:[13]

$$S = \sum_{\alpha \in P'} a_\alpha \langle -k_B \ln \rho_\alpha(\underline{\sigma}_\alpha) \rangle . \tag{2}$$

In the above equation k_B is the Boltzmann constant, $\underline{\sigma}_\alpha$ is the set of spin variables associated with the sites of the cluster α, $\rho_\alpha(\underline{\sigma}_\alpha)$ is the probability of the spin configuration $\underline{\sigma}_\alpha$ (in the cluster α), and finally a_α is the weight factor, which can be calculated using Moebius inversion;[13] the symbol $\langle \cdot \rangle$ means thermal average. We will refer to the set $\{\rho_\alpha(\underline{\sigma}_\alpha): \underline{\sigma}_\alpha \in \text{all possible spin configurations}\}$ as to the (reduced) density matrix of the cluster α.

We suppose that the maximal clusters are all of the same kind (in our case all square plaquettes) and that the global state of the system can be obtained repeating a single ''local'' state, defined by the density matrix of any maximal cluster α_0. In this case the entropy per site becomes

$$s = \frac{N_{\alpha_0}}{N} \sum_{\alpha \subseteq \alpha_0} a_\alpha b_\alpha \langle -k_B \ln \rho_\alpha(\underline{\sigma}_\alpha) \rangle , \tag{3}$$

where N_{α_0} is the number of maximal clusters in a lattice with N sites, and b_α is another weight factor which avoids counting more than once clusters contained in more than one maximal cluster.

Moreover the internal energy (per site) can be written as follows:

$$u=\frac{N_{\alpha_0}}{N}\langle h(\underline{\sigma}_{\alpha_0})\rangle \quad \text{with } \mathcal{H}=\sum_{\alpha_0} h(\underline{\sigma}_{\alpha_0}), \tag{4}$$

$\mathcal{H}$ being the Hamiltonian of the system. From now on we will omit the index α_0 (that is $\rho_{\alpha_0},\underline{\sigma}_{\alpha_0}$ become simply $\rho,\underline{\sigma}$).

Assuming implicitly that

$$\rho_\alpha(\underline{\sigma}_\alpha)=\sum_{\underline{\sigma}_{\alpha_0\setminus\alpha}} \rho(\underline{\sigma}), \quad \forall \alpha\subset\alpha_0 \tag{5}$$

(the symbol $\underline{\sigma}_{\alpha_0\setminus\alpha}$ denoting summation over all spin variables in α_0 except those in α), the free energy (per site) becomes a function of the maximal cluster density matrix ρ only, and so we will denote it by f_ρ. We can write

$$f_\rho=\frac{N_{\alpha_0}}{N}\sum_{\underline{\sigma}} \rho(\underline{\sigma})\left[h(\underline{\sigma})+k_BT\ln\frac{\rho(\underline{\sigma})}{\mu_\rho(\underline{\sigma})}\right], \tag{6}$$

where

$$\mu_\rho(\underline{\sigma})=\prod_{\alpha\subset\alpha_0}\rho_\alpha^{-a_\alpha b_\alpha}(\underline{\sigma}_\alpha) \tag{7}$$

and T is the absolute temperature. The summations in Eqs. (5) and (6), and the following ones too, run over all the plaquette spin configurations.

According to the CVM, the free energy f_ρ will be minimized with respect to the density matrix ρ, with the normalization constraint:

$$\sum_{\underline{\sigma}} \rho(\underline{\sigma})=1. \tag{8}$$

Looking for a constrained (normalized) stationary point one obtains the equations

$$\rho(\underline{\sigma})=e^{\beta\lambda_\rho}e^{-\beta h(\underline{\sigma})}\mu_\rho(\underline{\sigma}), \tag{9}$$

one for each plaquette spin configuration $\underline{\sigma}$. We have defined $\beta=1/k_BT$ and

$$e^{-\beta\lambda_\rho}=\sum_{\underline{\sigma}} e^{-\beta h(\underline{\sigma})}\mu_\rho(\underline{\sigma}). \tag{10}$$

In our case α_0 is a square plaquette and $\underline{\sigma}=(\sigma_1,\sigma_2,\sigma_3,\sigma_4)$. The actual expressions of $h(\underline{\sigma})$ and $\mu_\rho(\underline{\sigma})$ are

$$h(\underline{\sigma})=-\frac{J}{2}(\sigma_1\sigma_2+\sigma_2\sigma_3+\sigma_3\sigma_4+\sigma_4\sigma_1) -K(\sigma_1\sigma_3+\sigma_2\sigma_4)-L\sigma_1\sigma_2\sigma_3\sigma_4, \tag{11}$$

$$\mu_\rho(\underline{\sigma})=\frac{[\rho_{12}(\sigma_1,\sigma_2)\rho_{23}(\sigma_2,\sigma_3)\rho_{34}(\sigma_3,\sigma_4)\rho_{41}(\sigma_4,\sigma_1)]^{1/2}}{[\rho_1(\sigma_1)\rho_2(\sigma_2)\rho_3(\sigma_3)\rho_4(\sigma_4)]^{1/4}}. \tag{12}$$

The numbers 1,2,3,4 label the sublattices (and the sites of the plaquette belonging to them). 1-2, 2-3, 3-4, 4-1 are NN sites. So ρ_{ij} is the nearest-neighbor pair density matrix, while ρ_i is the single-site density matrix.

The system (9) can be numerically solved by using Kikuchi's natural iteration method;[21] it is possible to show that the solutions obtained by this method are always local minima of f_ρ.[21] When f_ρ has many local minima, these can be determined by choosing several different guess values for ρ. The solution will be the one which minimizes the free energy. Once the system (9) is solved we know the probability of each plaquette spin configuration $\rho(\sigma_1,\sigma_2,\sigma_3,\sigma_4)$ and so we can easily determine the order parameters in each sublattice:

$$m_i=\langle\sigma_i\rangle=\rho_i(+1)-\rho_i(-1) \tag{13}$$

as well as the two-site NN correlations:

$$R_{ij}=\langle\sigma_i\sigma_j\rangle =\rho_{ij}(+1,+1)-\rho_{ij}(+1,-1)-\rho_{ij}(-1,+1) +\rho_{ij}(-1,-1). \tag{14}$$

To conclude this section we would like to show an interesting property regarding the function λ_ρ which will be useful for further calculations. Looking for constrained (normalized) stationary points of this function one obtains the following equations:

$$\sum_{\underline{\sigma}'}\frac{\partial\ln\mu_\rho(\underline{\sigma}')}{\partial\rho(\underline{\sigma})}[\rho(\underline{\sigma}')-e^{\beta\lambda_\rho}e^{-\beta h(\underline{\sigma}')}\mu_\rho(\underline{\sigma}')]=0. \tag{15}$$

If ρ is a solution of Eq. (9) it is also a solution of Eq. (15) and so a stationary point of f_ρ is a stationary point for λ_ρ, too [let us remember that we always refer to constrained (normalized) stationary points]. The inverse implication is also true, provided the matrix $[\partial\ln\mu_\rho(\underline{\sigma}')/\partial\rho(\underline{\sigma})]_{\underline{\sigma},\underline{\sigma}'}$ is nonsingular. We must also recall[21] that, if ρ satisfies Eq. (9) [and hence Eq. (15)], then

$$f_\rho=\frac{N_{\alpha_0}}{N}\lambda_\rho. \tag{16}$$

Equations (15) and (16) will be useful in Sec. IV.

III. THE GROUND STATE AND QUALITATIVE RESULTS

In this section we will analyze the ground state phase diagram. The ground state can be easily determined by looking for the spin configurations of the maximal cluster which minimize the function h [see Eq. (4)], which we can call a ''maximal cluster (plaquette) Hamiltonian.'' In our case a configuration of the maximal cluster is specified by the values of the four spin variables lying on a square, and is denoted by $(\sigma_1,\sigma_2,\sigma_3,\sigma_4)$, where the indices refer to the four

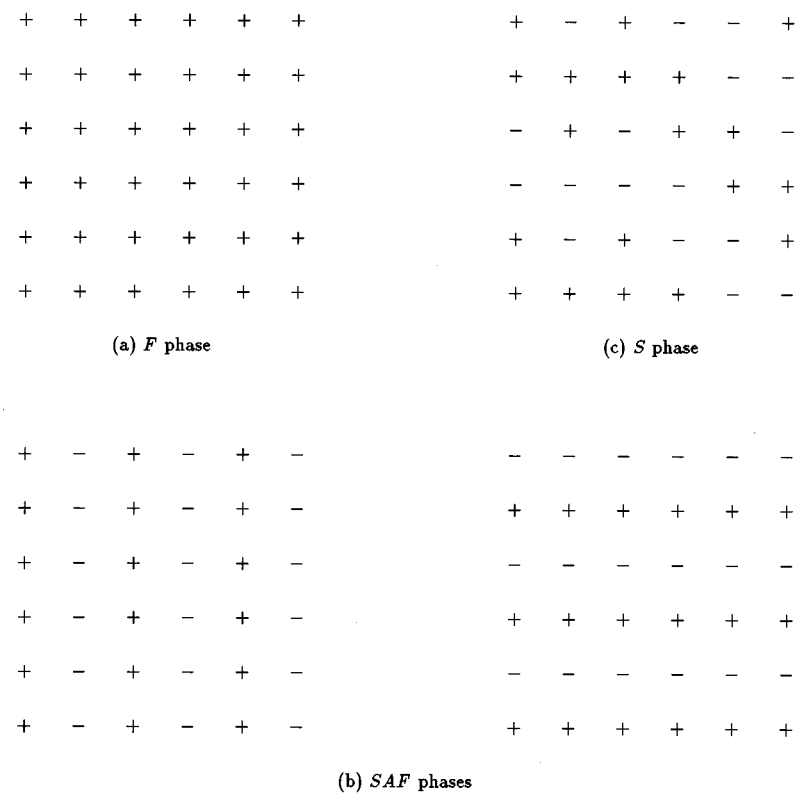

FIG. 1. Examples of ground states.

previously introduced sublattices. The only possible values of the spin variables are ± 1, which we will denote just with $\pm$. The possible ground state configurations are the following.

(1) The ferromagnetic state $(+,+,+,+)$ [or $(-,-,-,-)$ as well], which will be denoted by F (Fig. 1(a)). This state becomes antiferromagnetic [$(+,-,+,-)$ or $(-,+,-,+)$, denoted by AF] when J becomes $-J$. The corresponding values of the plaquette Hamiltonian are $h_{\mathrm{F}}=-2J-2K-L$ for the ferromagnetic configurations and $h_{\mathrm{AF}}=2J-2K-L$ for the antiferromagnetic ones.

(2) The so-called superantiferromagnetic states [Fig. 1(b)] $(+,+,-,-)$ and $(+,-,-,+)$ [or $(-,-,+,+)$ and $(-,+,+,-)$ as well], which will be denoted by SAF ($h_{\mathrm{SAF}}=2K-L$).

(3) A frustrated phase, where all the configurations with three + spins and one − spin (and vice versa) are allowed, and which we will call the S phase ($h_{\mathrm{S}}=L$).

Some more explanation is necessary about the S phase. Let us try to determine a spin configuration of the whole lattice such that all square plaquettes are in the S state [an example can be seen in Fig. 1(c)]. On each square the following condition must hold:

$$\sigma_1\sigma_2\sigma_3\sigma_4=-1 \tag{17}$$

(i.e., three + spins and one − spin or vice versa). Considering a lattice with $\mathcal{N}$ rows and $\mathcal{M}$ columns, one can choose freely the value (+ or −) of all spins in a given row and a given column, and the remaining spins are determined by Eq. (17). The degeneracy is then $2^{\mathcal{N}+\mathcal{M}-1}$ and the entropy per site vanishes in the thermodynamic limit.

Looking for the minimum of the values of the plaquette Hamiltonian h_{F}, h_{SAF}, h_{S} defined above, we can divide the normalized interaction plane $L/J,K/J$ in three regions, each corresponding to a different ground state (see Fig. 2).

Performing, by means of Eqs. (9)–(14), a numerical temperature analysis for significant values of the normalized interaction parameters we have recognized two ordered phases: a ferromagnetic one, characterized by order parameters:

$$m_1=m_2=m_3=m_4\equiv m \tag{18}$$

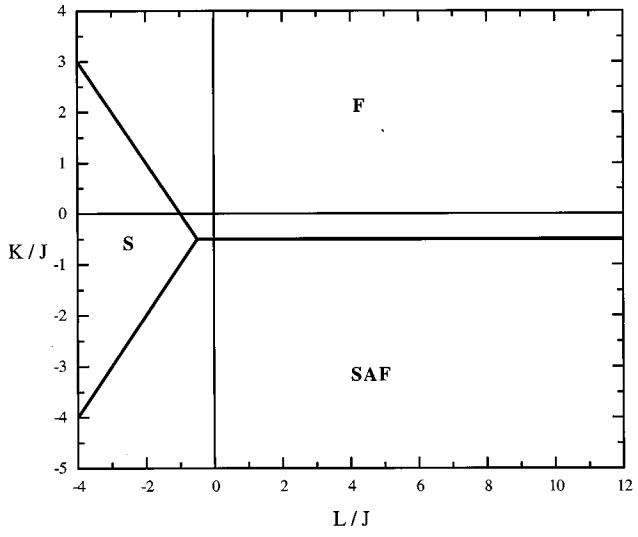

FIG. 2. Ground state phase diagram.

and a superantiferromagnetic one, characterized by

$$m_1 = m_2 = -m_3 = -m_4 \equiv m \tag{19}$$

or

$$m_1 = -m_2 = -m_3 = m_4 \equiv m \tag{20}$$

as well. These phases are a temperature evolution of the F and SAF ground states, respectively: for $K > -1/2$ we observe the symmetry property (18), while for $K < -1/2$ Eq. (19) or (20) holds. We will call ''column'' and ''row'' configurations the situations described by Eqs. (19) and (20), respectively, because the magnetizations of all sites lying on the same column (or row) of the lattice are equal (pairs 1-2 and 3-4 lie on columns).

In the S-phase region, when temperature is nonzero, we always have a paramagnetic solution, except reentrance phenomena near the boundary.

IV. HELPFUL HINTS FROM LANDAU THEORY

Let us now consider the temperature phase diagram. In order to obtain explicit equations for critical temperature and tricritical points we will make use of some concepts based on Landau theory.

In Landau hypotheses the free energy is an even function of an order parameter m, and is obviously dependent on the temperature and on the model's parameters, too. It is important to evaluate the second- (b) and fourth- (c) order derivatives of the free energy (with respect to m) in the point $m=0$, and to analyze their sign changes while temperature is varying. If, decreasing temperature, $b(T)$ becomes negative before $c(T)$ does, then we have a second-order transition and the transition temperature is determined by the equation $b(T)=0$; if on the contrary $c(T)$ becomes negative before $b(T)$, then we have a first-order transition. Finally, if $b(T)$ and $c(T)$ become negative at the same temperature, there we have a tricritical point.

We decided to apply this theory, substituting the free energy f_ρ with the function $\nu_\rho \equiv e^{-\beta\lambda_\rho}$, which has the same (normalized) stationary points and coincides with $e^{-\beta N f_\rho / N_{\alpha_0}}$ (N_{α_0}-th root of the partition function) if ρ is a (normalized) stationary point [see Eqs. (15) and (16)]. These properties assure that the function ν_ρ is completely equivalent to f_ρ, as far as the determination of the equilibrium density matrix and the critical and tricritical points is concerned. Using ν_ρ considerably simplifies our calculations because it depends only on the density matrices of the subclusters of the maximal cluster. In addition, when the maximal cluster is a square, the a_α coefficients associated with three-site and NNN two-site clusters vanish and so $e^{-\beta\lambda_\rho}$ depends on the NN pair and single-site density matrices only. Symmetry considerations allow one to further reduce the dimensionality of the problem.

In particular, in a ferromagnetic phase all NN pair density matrices are equal and so the NN two-site correlation coefficients [defined by Eq. (14)] are equal, too:

$$R_{12} = R_{23} = R_{34} = R_{41} \equiv R. \tag{21}$$

Then, satisfying the normalization constraint, ν_ρ can be rewritten as a function of the order parameter m [defined by Eq. (18)] and of the NN correlation coefficient R. Denoting this function by ν_F, we have

$$\begin{aligned}\nu_F(m,R) = {} & e^{-\beta h_F}(A_+^4 + A_-^4) + 4e^{-\beta h_S}(A_+^2 + A_-^2)B^2 \\ & + 4e^{-\beta h_{SAF}} A_+ A_- B^2 + 2e^{-\beta h_{AF}} B^4,\end{aligned} \tag{22}$$

where

$$A_\pm = \frac{(1+R\pm 2m)^{1/2}}{[8(1\pm m)]^{1/4}}, \quad B = \frac{(1-R)^{1/2}}{[8(1+m)]^{1/8}[8(1-m)]^{1/8}}.$$

On the contrary, in a superantiferromagnetic (SAF) phase, the NN two-site density matrices are equal in pairs: we can distinguish a ''row'' density matrix and a ''column'' density matrix, and so a ''row'' and a ''column'' correlation coefficient. They are, respectively, the density matrices (correlation coefficients) of a pair of nearest-neighbor spin variables lying on a row or on a column of the lattice. So we have

$$\begin{aligned} R_{12} &= R_{34} \equiv R_c, \\ R_{23} &= R_{41} \equiv R_r. \end{aligned} \tag{23}$$

Then ν_ρ can be rewritten as a function of the order parameter m [see Eqs. (19) and (20)] and of the two NN correlation coefficients R_r and R_c. Denoting this function by ν_{SAF}, we have

$$\begin{aligned}\nu_{\mathrm{SAF}}(m,R_c,R_r) = {} & 2e^{-\beta h_{\mathrm{F}}} A_{c+} A_{c-} B_r^2 \\ & + 4e^{-\beta h_{\mathrm{S}}}(A_{c+}A_{r+} + A_{c-}A_{r-}) B_c B_r \\ & + e^{-\beta h_{\mathrm{SAF}}}(A_{c+}^2 A_{r+}^2 + A_{c-}^2 A_{r-}^2 + 2B_c^2 B_r^2) \\ & + 2e^{-\beta h_{\mathrm{AF}}} A_{r+} A_{r-} B_c^2,\end{aligned} \tag{24}$$

where

$$A_{c\pm} = \frac{(1+R_c\pm 2m)^{1/2}}{[8(1\pm m)]^{1/4}}, \quad B_c = \frac{(1-R_c)^{1/2}}{[8(1+m)]^{1/8}[8(1-m)]^{1/8}},$$

$$A_{r\pm} = \frac{(1-R_r\pm 2m)^{1/2}}{[8(1\pm m)]^{1/4}}, \quad B_r = \frac{(1+R_r)^{1/2}}{[8(1+m)]^{1/8}[8(1-m)]^{1/8}}.$$

In both ferromagnetic and SAF cases we have a function $\nu(m,\underline{R})$, where $\underline{R}$ is a correlation parameter, which may be a two-component array. A stationary point of the function ν is defined by the following equations [let us remember that here we are interested in free (nonconstrained) stationary points, because the parameters m and $\underline{R}$ already account for the normalization constraint]:

$$\begin{aligned} &\frac{\partial \nu}{\partial m}(m,\underline{R}) = 0, \\ &\frac{\partial \nu}{\partial \underline{R}}(m,\underline{R}) = 0. \end{aligned} \tag{25}$$

The symbol $\partial/\partial\underline{R}$ is nothing but a gradient and so, if $\underline{R}$ is a two-component array, the second equation of Eq. (25) stands for two scalar equations. These equations define a (two-component) implicit function $\underline{\tilde{R}}(m)$; we can write

$$\underline{R}=\underline{\widetilde{R}}(m) \Leftrightarrow \frac{\partial \nu}{\partial \underline{R}}(m,\underline{R})=0. \tag{26}$$

So, in order to put ourselves in the Landau theory's conditions, we define the following function, too:

$$\widetilde{\nu}(m)\equiv \nu(m,\underline{\widetilde{R}}(m)). \tag{27}$$

This is a function of the order parameter m only, and it is possible to show that it is an even function. This is due to the fact that ν is even with respect to m; so $\partial\nu/\partial\underline{R}$ is even with respect to m, too, and then [definition (26)] $\underline{\widetilde{R}}(m)$ is an even function. Besides, it is easy to see that, if m is a stationary point for $\widetilde{\nu}$, then $(m,\underline{\widetilde{R}}(m))$ is a stationary point for ν, that is the system (25) is equivalent to the following one:

$$\frac{d\widetilde{\nu}}{dm}(m)=0,$$

$$\underline{R}=\underline{\widetilde{R}}(m). \tag{28}$$

So, if we want to determine stationary points of the free energy, we must look for stationary points of the (even) function $\widetilde{\nu}(m)$. According with Landau theory we are interested in the second- and fourth-order derivatives of $\widetilde{\nu}(m)$ when $m=0$. Observing that from definition (27) we have

$$\frac{d}{dm}=\frac{\partial}{\partial m}+\frac{d\underline{\widetilde{R}}}{dm}\cdot\frac{\partial}{\partial \underline{R}} \tag{29}$$

and remembering the parity considerations, we finally obtain

$$\frac{d^2\widetilde{\nu}}{dm^2}(0)=\frac{\partial^2\nu}{\partial m^2}(0,\underline{\widetilde{R}}(0)), \tag{30}$$

$$\frac{d^4\widetilde{\nu}}{dm^4}(0)=\frac{\partial^4\nu}{\partial m^4}(0,\underline{\widetilde{R}}(0))-3\frac{\partial^3\nu}{\partial m^2\partial \underline{R}}(0,\underline{\widetilde{R}}(0)) \times\left[\frac{\partial^2\nu}{\partial \underline{R}^2}(0,\underline{\widetilde{R}}(0))\right]^{-1}\frac{\partial^3\nu}{\partial m^2\partial \underline{R}}(0,\underline{\widetilde{R}}(0)). \tag{31}$$

The symbol $\partial^2/\partial\underline{R}^2$ indicates a double gradient (Hessian matrix). Let us observe that it is not necessary to know an explicit expression of $\underline{\widetilde{R}}(m)$ because we can evaluate its derivatives by using a multidimensional form of the implicit function theorem. In any case it is easy to derive the explicit expression of $\underline{\widetilde{R}}(0)$ by using definition (26). All the needed derivatives of ν can be calculated easily enough by using a truncated McLaurin series expansion with respect to m. Finally we obtain the derivatives (30) and (31) just as functions of temperature and the model's parameters. Their expressions are given in the Appendix. The equations

$$\frac{d^2\widetilde{\nu}}{dm^2}(0)=0,$$

$$\frac{d^4\widetilde{\nu}}{dm^4}(0)=0 \tag{32}$$

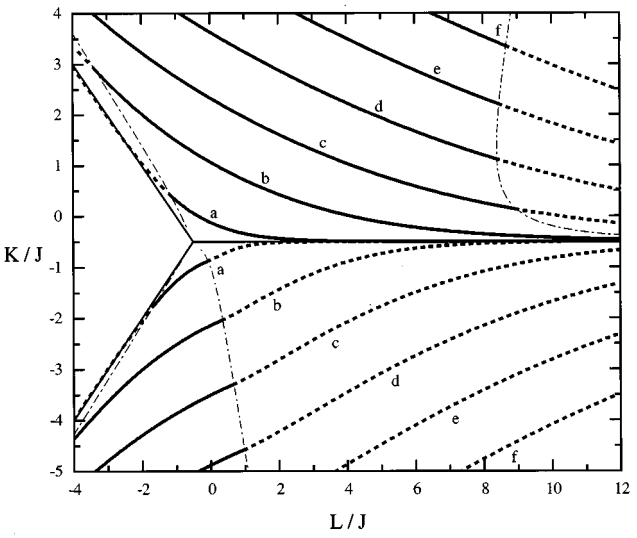

FIG. 3. Temperature phase diagram in the plane L/J,K/J: contour lines of transition temperature for $k_BT_c/J=2.0$ (a), 6.0 (b), 10.0 (c), 14.0 (d), 18.0 (e), 22.0 (f) (solid line, second-order transition; dotted line, first-order transition) and projections of the tricritical curves (dash-dotted lines).

can be numerically solved. The first equation of Eq. (32) determines the second-order transition temperature while together they give tricritical points.

V. DISCUSSION OF RESULTS AND COMPARISONS

Solving Eqs. (32) gives us a remarkable quantity of information about the phase diagram, at least within the limits of the square approximation. All the results are summed up in Figs. 3–5. Figure 3 displays some contour lines of transition temperature. These lines are composed by a second-order

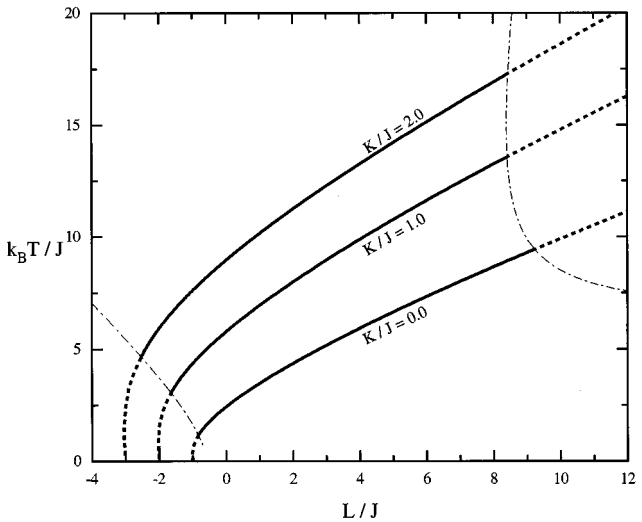

FIG. 4. Transition temperature vs L/J for several fixed values of $K/J>-1/2$ (solid line, second-order transition; dotted line, first-order transition) and projections of the tricritical curves (dash-dotted lines).

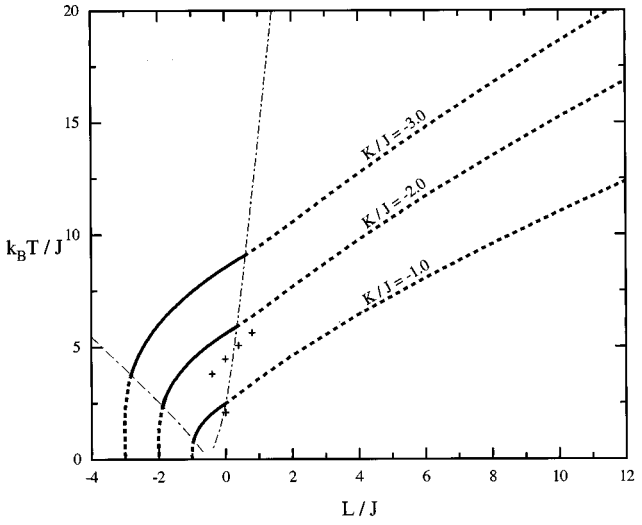

FIG. 5. Transition temperature vs L/J for several fixed values of $K/J<-1/2$ (solid line, second-order transition; dotted line, first-order transition) and projections of the tricritical curves (dash-dotted lines). Some critical points obtained in Ref. 18 are also reported (symbols +) for $K/J=-1$ (one point) and $K/J=-2$ (four points).

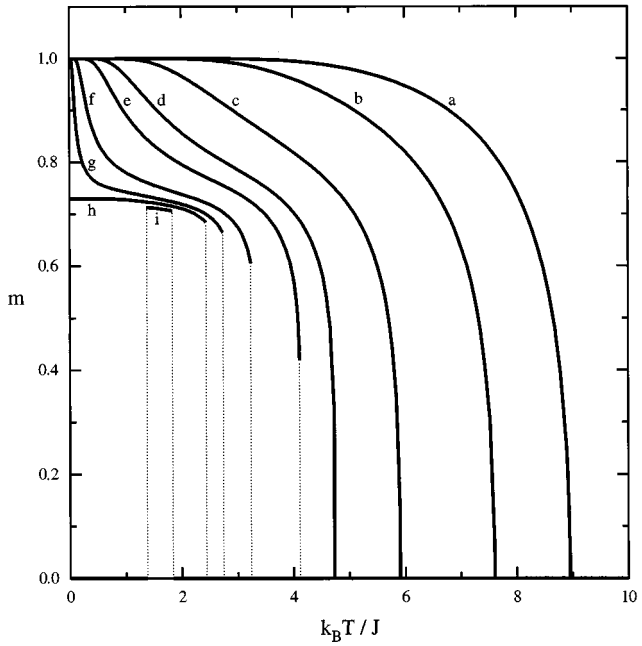

FIG. 6. Magnetization vs temperature for $K/J=2.0$ and $L/J=0.0$ (a), -1.0 (b), -2.0 (c), -2.5 (d), -2.7 (e), -2.9 (f), -2.97 (g), -3.0 (h), -3.03 (i) (ferromagnetic-paramagnetic transitions).

transition part (solid line), obtained by solving the first equation of Eq. (32), and by a first-order transition part (dotted line), evaluated in a completely numerical way. These two parts are separated by tricritical points. Different shapes of the first-order transition regions are obtained in the ferromagnetic and SAF cases. In the S-phase area we observe no contour line (except for the slightly reentrant lines coming from the F and SAF regions), that is the system is disordered at any nonzero temperature [except in the vicinity of the boundaries, where the behavior of magnetization is qualitatively that displayed in Fig. 6(i)]. Figures 4 and 5 show the transition temperature as a function of the parameter L/J for several fixed values of K/J. The behavior of this function is qualitatively similar in the ferromagnetic region (Fig. 4) and in the superantiferromagnetic one (Fig. 5). For negative decreasing L, the transition temperature gets lower; the system begins to present a first-order transition and then a slight reentrance phenomenon (in the S-phase region) which is enlarged if $|K|$ increases. For positive increasing L, the system exhibits a first-order transition, too, but the transition temperature gets higher. In the ferromagnetic region first-order transitions occur for higher positive values of L than in the superantiferromagnetic one. In Fig. 5 we have reported, as a comparison, some critical points obtained in Ref. 18 for $K/J=-1$ (1 point) and $K/J=-2$ (4 points). Figures 6 and 7 show the different behaviors of magnetization vs temperature. Figure 6 describes what happens when we approach (and enter) the S region from the F region (but the behavior is qualitatively the same if we come from the SAF region) for constant K and negative decreasing L. Figure 7 shows what happens for constant K and positive increasing L (in the SAF region). Particular attention must be paid at Fig. 6(h), which displays magnetization vs temperature in correspondence of the boundary between the F and S regions. Here the system presents a degeneracy, and we have $|m|<1$ even in the ground state $T=0$. The same behavior can be observed at the boundary between SAF and S regions, while at the boundary between F and SAF regions the magnetization vanishes at any nonzero temperature.

However the most remarkable fact we learn by looking at all the figures we have discussed is that first-order transitions occupy a very large part of the parameter space. We recover the results obtained in Ref. 11 for the case $L=0$. Moreover

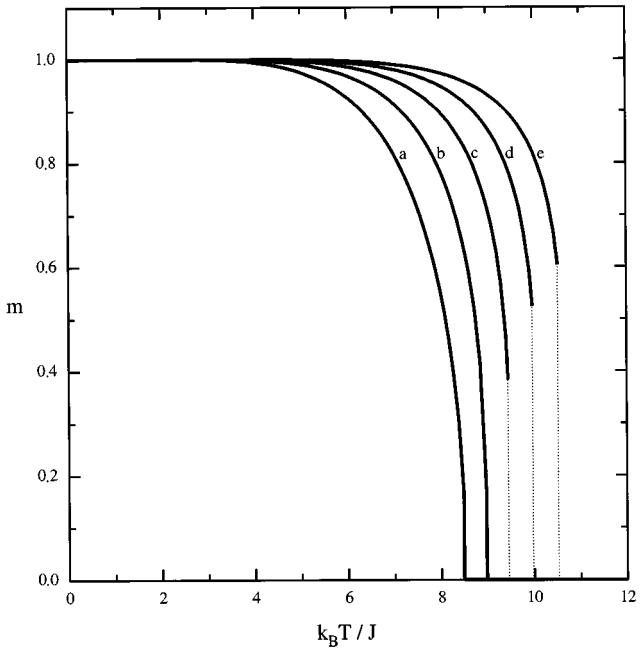

FIG. 7. Magnetization vs temperature for $K/J=-3.0$ and $L/J=0.0$ (a), 0.5 (b), 1.0 (c), 1.5 (d), 2.0 (e) (SAF-paramagnetic transitions).

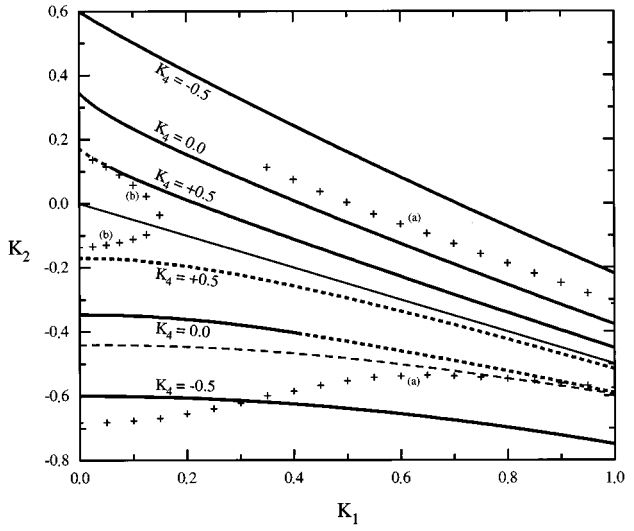

FIG. 8. Phase diagram in the K_1, K_2 plane: transition lines for several values of K_4 (solid line, second-order transition; dotted line, first-order transition). The thin solid straight line ($K_1+2K_2=0$) is the image of the line $K/J=-1/2$, which divides the F and SAF regions (F region in the upper part of the layer and SAF region in the lower one), while the dashed line in the SAF region is the $K_4=0$ transition line obtained by a Monte Carlo method (Ref. 5). Critical points obtained in Ref. 17 are also reported (symbols +) for $K_4=0.0$ (a) and $K_4=0.5$ (b).

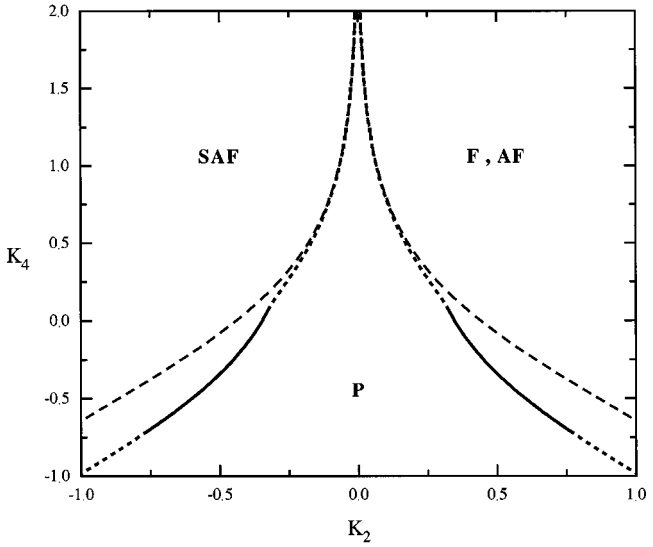

FIG. 9. $J=0$ ($K_1=0$) phase diagram in the K_2, K_4 plane (solid line, second-order transition; dotted line, first-order transition; dashed line, Baxter exact solution). The letter *P* stands for ''paramagnetic phase.''

we realize that the first-order transition area observed in Ref. 11 on the SAF side is just a subset of a larger two-dimensional first-order transition area. On the contrary, on the ferromagnetic side a first-order transition region occurs for higher values of L/J and so it cannot be ''seen'' at $L=0$.

In order to make some comparisons and consider the case $J=0$, we analyze the phase diagram in the parameter space $K_1=\beta J$, $K_2=\beta K$, $K_4=\beta L$. These are the parameters used in Ref. 17, where the same system as ours is studied by means of renormalization group methods, and in Ref. 5, where the model without plaquette interaction is studied by a Monte Carlo approach. The phase diagram is given in Fig. 8. The transition line obtained by the Monte Carlo method[5] in the SAF region is reported (dashed line), and must be compared with our $K_4=0$ transition line. There is a discrete similarity between these two lines, even if in the best matching region we have a first-order transition. We have also displayed (symbols ''+'') some critical points obtained in Ref. 17 but in this case the matching with our results is not very good.

The last step we have done is the model's analysis when $J=0$, which is very helpful to understand the errors introduced by the square approximation, because in this case we have in hand the exact solution (Baxter model[19,20]). Equations (32) become so easy that they can be explicitly solved, and there is a perfect symmetry between F (or AF) and SAF phases (let us observe that, when $J=0$, we have $h_F=h_{AF}$ and so the ordered phase may be either ferromagnetic or antiferromagnetic). The second-order transition line [solution of the first equation of Eq. (32)] is given by

$$K_4=-\frac{1}{2}\ln(e^{2|K_2|}-2e^{-2|K_2|}). \tag{33}$$

The above formula is valid only in an interval between two tricritical points [solutions of the system (32)]:

$$\frac{1}{4}\ln\left(\frac{25-\sqrt{313}}{2}\right)\leq|K_2|\leq\frac{1}{4}\ln\left(\frac{25+\sqrt{313}}{2}\right). \tag{34}$$

This critical line, together with the (numerically evaluated) first-order transition line and Baxter's critical line,

$$K_4=-\frac{1}{2}\ln\sinh(2|K_2|), \tag{35}$$

are reported in Fig. 9. It is worth noting that our transition line asymptotically coincides with Baxter's one in the limit $K_4\to\infty$ (the matching is already good for $K_4>0.5$), but in that region our solution predicts first-order transitions. The same result can be seen in Fig. 10, where the transition temperatures predicted by Baxter's solution and by our CVM solution are represented as a function of $L/|K|$. This result is quite disconcerting and deserves further investigations. It might be interesting to employ the CVM at higher order approximations in order to understand whether the first-order transition regions reduce or not.

VI. CONCLUSIONS

In this paper we have considered an Ising model on the square lattice with NN, NNN, and plaquette interactions, especially investigating the effects of the last one on the critical behavior of the system. We have carried out our investigation by using the CVM in the square approximation and characterized the phase diagram with full details, also developing a nearly analytical way to determine critical and tricritical points. This model, without plaquette interactions, was already studied with the CVM (at several increasing approximation orders) by Moran-Lopez *et al.*,[11] who obtained first-order transitions in a region of the model parameter space where other authors had found a nonuniversal critical behav-

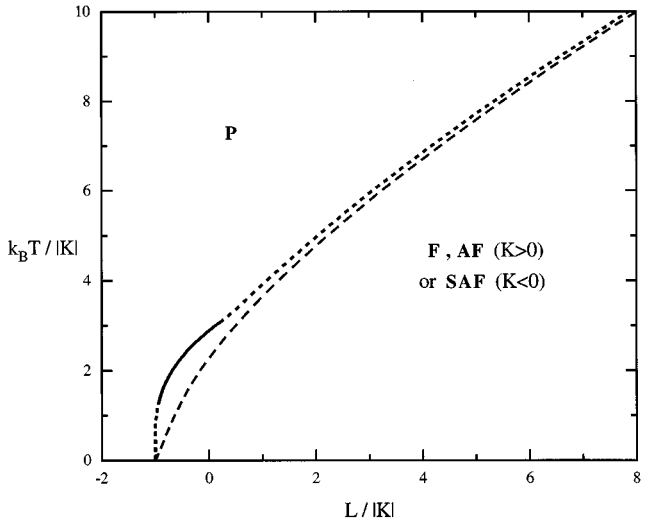

FIG. 10. $J=0$ phase diagram in the $L/|K|, k_BT/|K|$ plane (solid line, second-order transition; dotted line, first-order transition; dashed-line, Baxter exact solution). The ordered phase is ferromagnetic (or antiferromagnetic) when $K>0$ or superantiferromagnetic when $K<0$. The letter P stands for ''paramagnetic phase.''

ior. Our work shows how much the plaquette interaction term enlarges the first-order transition region. We have obtained several regions of the interaction parameter plane in which the system displays first-order (ferromagnetic-paramagnetic and SAF-paramagnetic) transitions, either for positive or negative values of the plaquette interaction parameter, with a slight reentrance effect in the last case. The first-order transition regions have been delimited by determining the tricritical lines. We have also observed that the local order of the frustrated phase (introduced by a negative plaquette interaction parameter) holds at zero temperature only: at finite temperature the system becomes paramagnetic. Among other comparisons, the one with the exactly solved Baxter model (vanishing NN interaction) is mainly interesting. We have pointed out some coincidence of the transition temperature for a region of the model parameters, even if in that region we find a first-order transition. The first-order transitions seem to be an effect of the approximation. In order to better understand the reliability of the CVM in the analysis of bidimensional systems (see, for example, Ref. 22), we think it might be useful to employ higher order approximations and to investigate whether and how the first-order transition regions are modified. We are going to carry on our work in this direction.

APPENDIX

In this Appendix we report the explicit expressions of the derivatives (30) and (31) for the ferromagnetic and SAF cases. In the ferromagnetic case we have

$$\frac{d^2\tilde{\nu}_{\rm F}}{dm^2}(0)=\frac{\partial^2\nu_{\rm F}}{\partial m^2}(0,R_0),$$

$$\frac{d^4\tilde{\nu}_{\rm F}}{dm^4}(0)=\frac{\partial^4\nu_{\rm F}}{\partial m^4}(0,R_0)-3\left(\frac{\partial^3\nu_{\rm F}}{\partial m^2\partial R}(0,R_0)\right)^2\Bigg/\frac{\partial^2\nu_{\rm F}}{\partial R^2}(0,R_0),$$

where

$$R_0=\frac{-e^{-\beta h_{\rm F}}+e^{-\beta h_{\rm AF}}}{e^{-\beta h_{\rm F}}-4e^{-\beta h_{\rm S}}-2e^{-\beta h_{\rm SAF}}+e^{-\beta h_{\rm AF}}}$$

and

$$\frac{\partial^2\nu_{\rm F}}{\partial m^2}(0,R)=\frac{1}{2}e^{-\beta h_{\rm F}}(1-R)^2-\frac{1}{4}e^{-\beta h_{\rm S}}(3-5R)(1-R)-\frac{1}{2}e^{-\beta h_{\rm SAF}}\frac{(3+R)(1-R)^2}{(1+R)}+\frac{1}{4}e^{-\beta h_{\rm AF}}(1-R)^2,$$

$$\frac{\partial^4\nu_{\rm F}}{\partial m^4}(0,R)=6e^{-\beta h_{\rm F}}(1-R)^2-\frac{3}{16}e^{-\beta h_{\rm S}}(45-67R)(1-R)-\frac{3}{2}e^{-\beta h_{\rm SAF}}\frac{(7+6R+3R^2)(3+R)(1-R)^2}{(1+R)^3}+\frac{9}{4}e^{-\beta h_{\rm AF}}(1-R)^2,$$

$$\frac{\partial^2\nu_{\rm F}}{\partial R^2}(0,R)=\frac{1}{2}e^{-\beta h_{\rm F}}-2e^{-\beta h_{\rm S}}-e^{-\beta h_{\rm SAF}}+\frac{1}{2}e^{-\beta h_{\rm AF}},$$

$$\frac{\partial^3\nu_{\rm F}}{\partial m^2\partial R}(0,R)=-e^{-\beta h_{\rm F}}(1-R)+\frac{1}{2}e^{-\beta h_{\rm S}}(4-5R)+e^{-\beta h_{\rm SAF}}\frac{(4+3R+R^2)(1-R)}{(1+R)^2}-\frac{1}{2}e^{-\beta h_{\rm AF}}(1-R).$$

In the SAF case it is useful to substitute the parameters R_r and R_c with $\overline{R}$ and ΔR, defined as follows:

$$\overline{R}=\frac{R_c+R_r}{2},$$

$$\Delta R=\frac{R_c-R_r}{2}. \tag{A1}$$

In this way the Hessian matrix in Eq. (31) becomes diagonal. We have

$$\frac{d^2\tilde{\nu}_{\mathrm{SAF}}}{dm^2}(0)=\frac{\partial^2\nu_{\mathrm{SAF}}}{\partial m^2}(0,\overline{R}_0,\Delta R_0),$$

$$\frac{d^4\tilde{\nu}_{\mathrm{SAF}}}{dm^4}(0)=\frac{\partial^4\nu_{\mathrm{SAF}}}{\partial m^4}(0,\overline{R}_0,\Delta R_0)-3\left[\frac{\partial^3\nu_{\mathrm{SAF}}}{\partial m^2\partial\overline{R}}(0,\overline{R}_0,\Delta R_0)\right]^2\Bigg/\frac{\partial^2\nu_{\mathrm{SAF}}}{\partial\overline{R}^2}(0,\overline{R}_0,\Delta R_0)$$
$$-3\left[\frac{\partial^3\nu_{\mathrm{SAF}}}{\partial m^2\partial\Delta R}(0,\overline{R}_0,\Delta R_0)\right]^2\Bigg/\frac{\partial^2\nu_{\mathrm{SAF}}}{\partial\Delta R^2}(0,\overline{R}_0,\Delta R_0),$$

where $\overline{R}_0=R_0$, $\Delta R_0=0$, and

$$\frac{\partial^2\nu_{\mathrm{SAF}}}{\partial m^2}(0,\overline{R},0)=-\frac{1}{4}e^{-\beta h_{\mathrm{F}}}(3+\overline{R})(1-\overline{R})-\frac{1}{4}e^{-\beta h_{\mathrm{S}}}\frac{3+18\overline{R^2}-5\overline{R^4}}{1-\overline{R^2}}+\frac{3}{4}e^{-\beta h_{\mathrm{SAF}}}(1-\overline{R^2})-\frac{1}{4}e^{-\beta h_{\mathrm{AF}}}(3-\overline{R})(1+\overline{R}),$$

$$\frac{\partial^4\nu_{\mathrm{SAF}}}{\partial m^4}(0,\overline{R},0)=-\frac{3}{4}e^{-\beta h_{\mathrm{F}}}\frac{(3+\overline{R})(1-\overline{R})(7+6\overline{R}+3\overline{R^2})}{(1+\overline{R})^2}-\frac{3}{16}e^{-\beta h_{\mathrm{S}}}\frac{45+1372\overline{R^2}-386\overline{R^4}+316\overline{R^6}-67\overline{R^8}}{(1-\overline{R^2})^3}$$
$$+\frac{33}{4}e^{-\beta h_{\mathrm{SAF}}}(1-\overline{R^2})-\frac{3}{4}e^{-\beta h_{\mathrm{AF}}}\frac{(3-\overline{R})(1+\overline{R})(7-6\overline{R}+3\overline{R^2})}{(1-\overline{R})^2},$$

$$\frac{\partial^2\nu_{\mathrm{SAF}}}{\partial\overline{R^2}}(0,\overline{R},0)=\frac{1}{2}e^{-\beta h_{\mathrm{F}}}-2e^{-\beta h_{\mathrm{S}}}-e^{-\beta h_{\mathrm{SAF}}}+\frac{1}{2}e^{-\beta h_{\mathrm{AF}}},$$

$$\frac{\partial^3\nu_{\mathrm{SAF}}}{\partial m^2\partial\overline{R}}(0,\overline{R},0)=\frac{1}{2}e^{-\beta h_{\mathrm{F}}}(1+\overline{R})-\frac{1}{2}e^{-\beta h_{\mathrm{S}}}\frac{21\overline{R}-10\overline{R^3}+5\overline{R^5}}{(1-\overline{R^2})^2}-\frac{3}{2}e^{-\beta h_{\mathrm{SAF}}}\overline{R}-\frac{1}{2}e^{-\beta h_{\mathrm{AF}}}(1-\overline{R}),$$

$$\frac{\partial^2\nu_{\mathrm{SAF}}}{\partial\Delta\overline{R^2}}(0,\overline{R},0)=-\frac{1}{2}e^{-\beta h_{\mathrm{F}}}-2e^{-\beta h_{\mathrm{S}}}\frac{1+\overline{R^2}}{1-\overline{R^2}}+e^{-\beta h_{\mathrm{SAF}}}-\frac{1}{2}e^{-\beta h_{\mathrm{AF}}},$$

$$\frac{\partial^3\nu_{\mathrm{SAF}}}{\partial m^2\partial\Delta\overline{R}}(0,\overline{R},0)=2e^{-\beta h_{\mathrm{F}}}\frac{1}{1+\overline{R}}+2e^{-\beta h_{\mathrm{S}}}\frac{1+8\overline{R^2}-\overline{R^4}}{(1-\overline{R^2})^2}-\frac{3}{2}e^{-\beta h_{\mathrm{SAF}}}+2e^{-\beta h_{\mathrm{AF}}}\frac{1}{1-\overline{R}}.$$

These are the formulas we used for numeric computation of second-order transition temperatures and tricritical points, following the method described in Sec. IV.

[1] M. P. Nightingale, Phys. Lett. **59A**, 468 (1977).
[2] M. N. Barber, J. Phys. A **12**, 679 (1979).
[3] F. Y. Wu, Phys. Rev. B **4**, 2312 (1971).
[4] J. Oitmaa, J. Phys. A **14**, 1159 (1981).
[5] R. H. Swendsen and S. Krinsky, Phys. Rev. Lett. **43**, 177 (1979).
[6] D. P. Landau, Phys. Rev. B **21**, 1285 (1980).
[7] K. Binder and D. P. Landau, Phys. Rev. B **21**, 1941 (1980).
[8] D. P. Landau and K. Binder, Phys. Rev. B **31**, 5946 (1985).
[9] K. Tanaka, T. Horiguchi, and T. Morita, Phys. Lett. A **165**, 266 (1992).
[10] J. L. Moran-Lopez, F. Aguilera-Granja, and J. M. Sanchez, Phys. Rev. B **48**, 3519 (1993).
[11] J. L. Moran-Lopez, F. Aguilera-Granja, and J. M. Sanchez, J. Phys. Condens. Matter **6**, 9759 (1994).
[12] R. Kikuchi, Phys. Rev. **81**, 988 (1951).
[13] G. An, J. Stat. Phys. **52**, 727 (1988).
[14] T. Morita, J. Stat. Phys. **59**, 819 (1990)
[15] M. Nauenberg and B. Nienhuis, Phys. Rev. Lett. **33**, 944 (1974).
[16] J. M. J. van Leeuwen, Phys. Rev. Lett. **34**, 1056 (1975).
[17] F. Lee, H. H. Chen, and F. Y. Wu, Phys. Rev. B **40**, 4871 (1989).
[18] K. Minami and M. Suzuki, Physica A **195**, 457 (1993).
[19] R. J. Baxter, Ann. Phys. (N.Y.) **70**, 193 (1972).
[20] L. P. Kadanoff and F. J. Wegner, Phys. Rev. B **4**, 3989 (1971).
[21] R. Kikuchi, J. Chem. Phys. **60**, 1071 (1974).
[22] T. Morita, Physica A **141**, 335 (1987).